Talanta 84 (2011) 71–77

Contents lists available at ScienceDirect

Talanta

journal homepage: www.elsevier.com/locate/talanta

Amperometric hydrogen peroxide biosensor based on the immobilization of heme proteins on gold nanoparticles–bacteria cellulose nanofibers nanocomposite

Wei Wang, Tai-Ji Zhang, De-Wen Zhang, Hong-Yi Li, Yu-Rong Ma, Li-Min Qi, Ying-Lin Zhou*, Xin-Xiang Zhang*

Beijing National Laboratory for Molecular Sciences (BNLMS), Key Laboratory of Biochemistry and Molecular Engineering, College of Chemistry, Peking University, Beijing 100871, PR China

ARTICLE INFO

Article history:
Received 2 September 2010
Received in revised form 2 December 2010
Accepted 8 December 2010
Available online 15 December 2010

Keywords:
Bacteria cellulose
Gold nanoparticles
Horseradish peroxidase
Hemoglobin
Myoglobin
Biosensor

ABSTRACT

A novel matrix, gold nanoparticles–bacterial cellulose nanofibers (Au–BC) nanocomposite was developed for enzyme immobilization and biosensor fabrication due to its unique properties such as satisfying biocompatibility, good conductivity and extensive surface area, which were inherited from both gold nanoparticles (AuNPs) and bacterial cellulose nanofibers (BC). Heme proteins such as horseradish peroxidase (HRP), hemoglobin (Hb) and myoglobin (Mb) were successfully immobilized on the surface of Au–BC nanocomposite modified glassy carbon electrode (GCE). The immobilized heme proteins showed electrocatalytic activities to the reduction of H_2O_2 in the presence of the mediator hydroquinone (HQ), which might be due to the fact that heme proteins retained the near-native secondary structures in the Au–BC nanocomposite which was proved by UV–vis and IR spectra. The response of the developed biosensor to H_2O_2 was related to the amount of AuNPs in Au–BC nanocomposite, indicating that the AuNPs in BC network played an important role in the biosensor performance. Under the optimum conditions, the biosensor based on HRP exhibited a fast amperometric response (within 1 s) to H_2O_2, a good linear response over a wide range of concentration from 0.3 μM to 1.00 mM, and a low detection limit of 0.1 μM based on $S/N = 3$. The high performance of the biosensor made Au–BC nanocomposite superior to other materials as immobilization matrix.

1. Introduction

Since biosensors with electrochemical analysis are of great importance in many fields, they have attracted much attention for the construction with high selectivity and sensitivity [1,2]. Enzyme immobilization is very important in biosensor development. The kinetics, stability and specificity of immobilized enzyme perhaps differ from that of the enzyme in homogeneous solution due to the structural change in immobilization. Therefore, the construction of the immobilized enzyme layer which can retain its specific biological function is highly desired [3]. Different biocompatible materials such as conducting polymers [4–6], sol–gel materials [7–10], nanomaterials [11–13], and nanocomposite materials [14–16] for the immobilizations and biosensing applications of enzymes have been proposed. Cai et al. [17] synthesized gold nanoparticle–$CaCO_3$ hybrid material (AuNP–$CaCO_3$) to fabricate horseradish peroxidase (HRP)–AuNP–$CaCO_3$ bioconjugates, which were embedded into a silica sol–gel matrix to construct a novel biosensor. And Liu et al. [18] developed a kind of nanocomposites with good dispersion in water through non-covalent adsorption of toluidine blue on multi-walled carbon nanotubes for electric communication between HRP and electrode.

As biosynthesized cellulose, bacterial cellulose (BC) is a kind of extracellular cellulose produced by acetic acid bacteria *Acetobacter xylinum* [19]. BC is an unbranched polymer of β-1,4-linked glucopyranose residues and composed of self-entangled ultra-fine fibrils with width less than 100 nm, which has a three dimensional nano-network structure with a distinct tunnel and pore structure [19,20]. Because of its characteristic microstructure, BC presents unique properties such as high purity, high crystallinity, high tensile strength, elasticity, excellent biodegradability, excellent biological affinity, biocompatibility and extensive surface area [21–23]. Benefiting from its unique properties, BC has attracted increasing interest in commercial applications over the past few years as materials for industry (paper, headphone membranes, food and textiles) and biomaterials including temporary skin substitute, artificial blood vessels, and nerves [24–27]. However, there

* Corresponding authors. Tel.: +86 10 62754680; fax: +86 10 62754680.
E-mail addresses: zhouyl@pku.edu.cn (Y.-L. Zhou), zxx@pku.edu.cn (X.-X. Zhang).

0039-9140/$ – see front matter © 2010 Elsevier B.V. All rights reserved.
doi:10.1016/j.talanta.2010.12.015

are few applications and studies of BC in biosensors up to now. Liang et al. [28] reported that carbonized nanofiber BC could be used to fabricate BC-based carbon paste electrode which has excellent electrocatalytic activity to the reduction of nitrite. As a kind of biocompatible material with unique properties, BC should be a very suitable matrix for enzyme immobilization.

Gold nanoparticles (AuNPs) have also been applied as the film forming material to construct different kinds of films with redox proteins on electrodes because of their good biocompatibility and conductivity [29,30], which could provide an environment that is similar to the nature for enzyme immobilization [31,32]. Moreover, the nanoparticles could act as tiny conduction centers to facilitate electron transfer [33,34].

The excellent properties of both BC and AuNPs inspired us to combine them into a nanocomposite and use it as a novel matrix to immobilize proteins on the electrode surface. In our recent work, novel Au–BC nanocomposite was first prepared via a facile one-step biotemplated method in aqueous suspension using poly(ethyleneimine) (PEI) as reducing and linking agent, and HRP was successfully embedded into the nano-network structure of the Au–BC nanocomposite while remaining its bioactivity [35]. Au–BC nanocomposite was functioned as a superior immobilization matrix for HRP than individual BC and AuNPs.

In this work, Au–BC nanocomposite was used to immobilize two other heme proteins, Hb and Mb, to see if this novel nanocomposite was suitable to immobilize proteins with different sizes, and the performance of these proteins including HRP in Au–BC nanocomposite was investigated in details. The electrocatalytic activities of heme proteins immobilized on the Au–BC nanocomposite modified GCE were investigated in the presence of hydroquinone (HQ). The conformation of the proteins in the films was characterized by UV–vis and IR spectra. The effect of the amount of AuNPs in the Au–BC nanocomposite on the sensitivity of biosensor to H_2O_2 was also studied. The catalytic activities of the biosensor based on heme protein/Au–BC to the reduction of H_2O_2 were evaluated by amperometry.

2. Experimental

2.1. Reagents

Horseradish peroxidase (HRP) and myoglobin (Mb, from equine skeletal muscle) were purchased from Sigma. Hemoglobin (Hb, from bovine erythrocytes) was purchased from Merck. Poly(ethylenimine) (M_w = 25,000), potassium ferricyanide ($K_3Fe(CN)_6$) and potassium ferrocyanide ($K_4Fe(CN)_6$) were obtained from Aldrich. Hydrochloroauric acid trihydrate ($HAuCl_4{\cdot}3H_2O$, 99.9%), isopropanol and hydrogen peroxide (H_2O_2) were purchased from Beijing Chemical Reagent Company (Beijing, China), and hydroquinone (HQ) was purchased from Sinopharm Chemical Reagent Co. (Shanghai, China). All chemicals were of analytical grade and used without further purification. Double distilled water (ddH_2O) was used and all the solutions were freshly prepared.

$[Fe(CN)_6]^{3-/4-}$ redox probe solution was prepared as follows: the $K_3Fe(CN)_6/K_4Fe(CN)_6$ (1:1, 1 mM) mixture was dissolved in 0.1 M phosphate buffer (pH 7.4), and 0.1 M KCl was added as the supporting electrolyte.

2.2. Synthesis of Au–BC nanocomposite

The BC pellicle was obtained as reported in Ref. [36] and was disrupted into nanofibers aqueous suspension by Ultrasonic Cell Disruption System at room temperature. Au–BC nanocomposite was synthesized by the reduction of $HAuCl_4$ with PEI in aqueous mixed BC nanofibers solution as reported in Ref.[35]. The main procedures were as following: 0.5 mL of 10 g/L PEI aqueous solution and 4.25 mL aqueous suspension containing ~0.02 mg/mL BC nanofibers were first mixed together and stirred for 30 min at room temperature. After adding 0.25 mL of 20 mM $HAuCl_4$, the mixed suspension was kept at 60 °C under static condition for 1 h, leading to the formation of Au–BC nanocomposite. The product was collected by centrifugation and washed thoroughly with ddH_2O.

2.3. Preparation of modified electrodes

Glassy carbon electrode (GCE) was polished with 0.05 μm alumina slurry by a polisher and then washed in ddH_2O and ethanol for 3 min by an ultrasonic cleaner. The pretreated GCE was coated by casting 5 μL of the above Au–BC suspension and dried at room temperature (25 °C). This modified electrode was denoted as Au–BC/GCE. Then, the Au–BC/GCE was casted with 5 μL HRP solution (3 mg/mL, phosphate buffer), 5 μL Hb solution (3 mg/mL, phosphate buffer), or 5 μL Mb solution (3 mg/mL, phosphate buffer), respectively, for an incubation period of 12 h at 4 °C. The modified electrode was washed gently with ddH_2O three times and then stored in phosphate buffer at 4 °C. These modified electrodes were denoted as HRP/Au–BC/GCE, Hb/Au–BC/GCE and Mb/Au–BC/GCE, respectively. Similarly, BC modified GCE (BC/GCE) and HRP/BC modified GCE (HRP/BC/GCE) were also prepared by this method. The modified electrodes were gently washed three times with phosphate buffer and ddH_2O before each measurement.

2.4. Apparatus and measurements

All electrochemical measurements were carried out on a CHI 660C (CH Instruments, Shanghai, China) electrochemical workstation. A conventional three-electrode system with the modified electrodes obtained via the above methods as the working electrode, a platinum wire (radius 0.5 mm) as the counter electrode, and an Ag/AgCl (3 M KCl) electrode as the reference electrode was used throughout at room temperature (25 °C). The cyclic voltammetric measurements were taken in an unstirred electrochemical cell. Amperometric curves were obtained by consequently adding H_2O_2 solution with a certain concentration into phosphate buffer solution containing 0.5 mM HQ at −0.15 V. A magnetic Teflon stirrer provided the convective transport during the amperometric measurements. To eliminate dissolved oxygen, all the solutions used above were bubbled by highly pure argon for 15 min before experiments, and then the argon atmosphere was kept over the solutions through the experiments.

UV–vis spectroscopies were obtained by a UV–vis spectrophotometer (Cary E1, Varian). Reflectance absorption infrared (RAIR) spectra were taken on Nicolet MAGNA-IR 750 (Nicolet) at room temperature. The films of proteins, Au–BC and protein/Au–BC for spectroscopy were prepared on quartz slides (for UV–vis) or silicon substrates (for RAIR) in a similar method as in the preparation of the modified electrodes.

3. Results and discussion

3.1. Characterization of Au–BC nanocomposite

The preparation of the Au–BC nanocomposite was discussed in details in our recent work [35]. Herein, a general introduction about the preparation and characterization of the Au–BC was given for the readers to have a basic understanding about this kind of biocomposites. Bacteria usually produce soft and semitransparent BC pellicles comprised of nanofibers. Before assembling AuNPs to these nanofibers, the BC pellicles were first disrupted into nanofibers aqueous suspension. The scanning electron microscopy

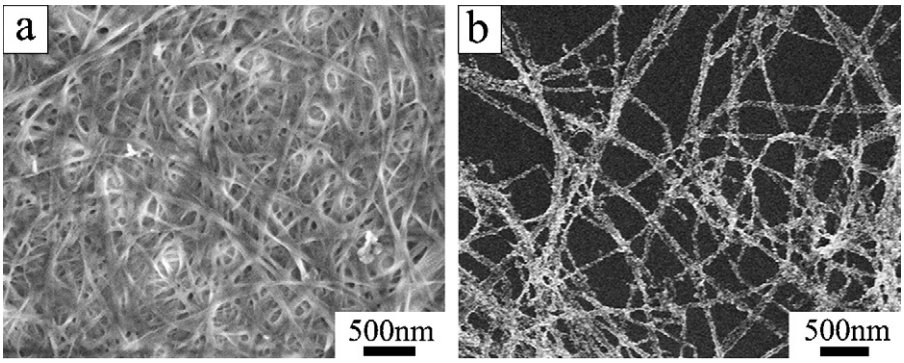

Fig. 1. The SEM images of (a) BC nanofibers and (b) Au–BC nanocomposite.

(SEM) image of BC nanofibers was shown in Fig. 1a. The BC nanofibers were ribbon-shaped, about 40 nm in size and form nano-network structure. BC nanofibers were colorless and turned to purple after coating AuNPs, which meant AuNPs were assembled onto BC nanofibers. The SEM image of the obtained Au–BC nanocomposite was shown in Fig. 1b. The BC nanofibers remained their nano-network structure after coating with AuNPs (~9 nm) uniformly. The Au–BC nanocomposite was about 60 nm in size, a little larger than the diameter of BC nanofibers.

3.2. Electrochemical characterization of modified electrodes

The Au–BC nanocomposite was a promising matrix for enzyme loading and biosensing which inherited advantages from its parent materials, such as excellent biological affinity, satisfying biocompatibility, extensive surface area and good conductivity. Cyclic voltammetry (CV) of $[Fe(CN)_6]^{3-/4-}$ is a valuable and convenient tool to test the kinetic barrier of the interface. It was chosen as a marker to investigate the changes of electrode behavior after each assembly step to see whether Au–BC nanocomposite could be used to immobilize different heme proteins including HRP, Hb and Mb. Fig. 2 showed cyclic voltammetries (CVs) of different modified electrodes in 1.0 mM $[Fe(CN)_6]^{3-/4-}$ solution. The CV curve of bare GCE showed one pair of quasi reversible and well-defined redox peaks with the peak-to-peak separation (ΔE_p) of 73 mV (Fig. 2a), indicating a fast and direct electron transfer reaction occurred. After casting the BC on the bare GCE, both the cathodic and the anodic peak currents decreased obviously and the ΔE_p increased to 199 mV (Fig. 2b). It was mainly due to the poor conductivity of BC nanofibers, which acted as the inert electron and mass transfer blocking layer, and hindered the diffusion of $[Fe(CN)_6]^{3-/4-}$ toward the electrode surface. Compared to BC/GCE, the peak current of Au–BC/GCE increased greatly, accompanying the decrease of peak-to-peak separation (Fig. 2c). The CV curve of Au–BC/GCE was almost identical to that of bare GCE, indicating the conductivity of Au–BC was greatly improved compared to BC itself. The reason was that AuNPs were directly attached to the surface of the BC nanofibers and formed a continuous array of gold nanoparticles on the electrode, which facilitated the electron transfer between the $[Fe(CN)_6]^{3-/4-}$ and the electrode surface. After incubating Au–BC/GCE with different protein solutions, the decreases of the peak currents was observed for all the three protein/Au–BC modified electrodes (Fig. 2d, e and f), which was strong evidence that all these proteins were successfully embedded in the Au–BC nanocomposite film and the presence of proteins decreased the effective electrode areas, leading to the decrease of the peak currents.

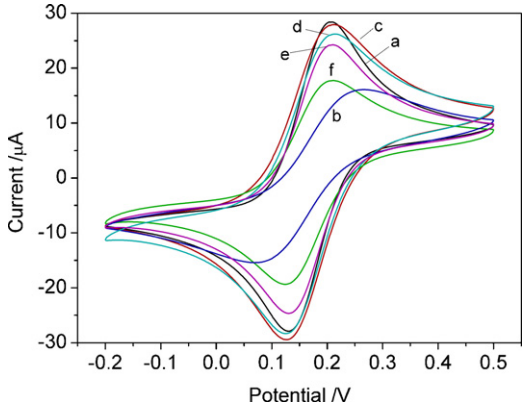

Fig. 2. Cyclic voltammograms of (a) bare GCE; (b) BC/GCE; (c) Au–BC/GCE; (d) HRP/Au–BC/GCE; (e) Mb/Au–BC/GCE and (f) Hb/Au–BC/GCE in 1 mM $[Fe(CN)_6]^{3-/4-}$ + 0.1 M KCl as the supporting electrolyte at a scan rate of 100 mV/s.

3.3. Electrocatalytic activity of heme proteins immobilized on the Au–BC nanocomposite modified GCE

In order to investigate the bioactivity of immobilized heme proteins on Au–BC nanocomposite, the developed biosensors were used for the determination of H_2O_2. HQ is often used as an electron mediator to investigate the bioactivity of heme proteins because the direct electrochemistry of heme proteins is not easily observed [37,38]. The CV of Hb/Au–BC/GCE in phosphate buffer solution containing 0.5 mM HQ was shown in Fig. S1 (see electronic supplementary materials, E.S.M.). In the absence of H_2O_2, a pair of redox peaks, characteristic of a diffusion-limited redox process, was observed at the Hb/Au–BC/GCE (Fig. S1a), which indicated HQ could effectively exchange electrons through Hb/Au–BC film on the electrode surface. After the addition of 0.5 mM H_2O_2, the significant increase of the reduction peak, accompanied by a decrease of the oxidation peak, was observed (Fig. S1b). Further the addition of H_2O_2 in the buffer caused a further increase of the reduction peak and the decrease of the oxidation peak (Fig. S1c). However, H_2O_2 had little effect on the peak currents of HQ at the Au–BC/GCE. These results demonstrated that there existed reactions among Hb, H_2O_2 and HQ at the Hb/Au–BC/GCE. The increase of reduction current response to H_2O_2 at Hb/Au–BC/GCE was mainly due to the biocatalytic effect of Hb. The reason might be that both the nano-network BC structure and the AuNPs provided an excellent biocompatible environment for Hb on the electrode surface, which retained its bioactivity well and catalyzed the reaction with H_2O_2 and HQ. Mb/Au–BC and HRP/Au–BC films also showed similar biocatalytic behaviors toward H_2O_2.

The cyclic voltammograms of Hb/Au–BC/GCE in phosphate buffer (pH 7.4) containing 0.5 mM HQ and 0.5 mM H_2O_2 at different scan rates were investigated. Both of anodic and of cathodic peak currents were linearly correlated to the square root of scan

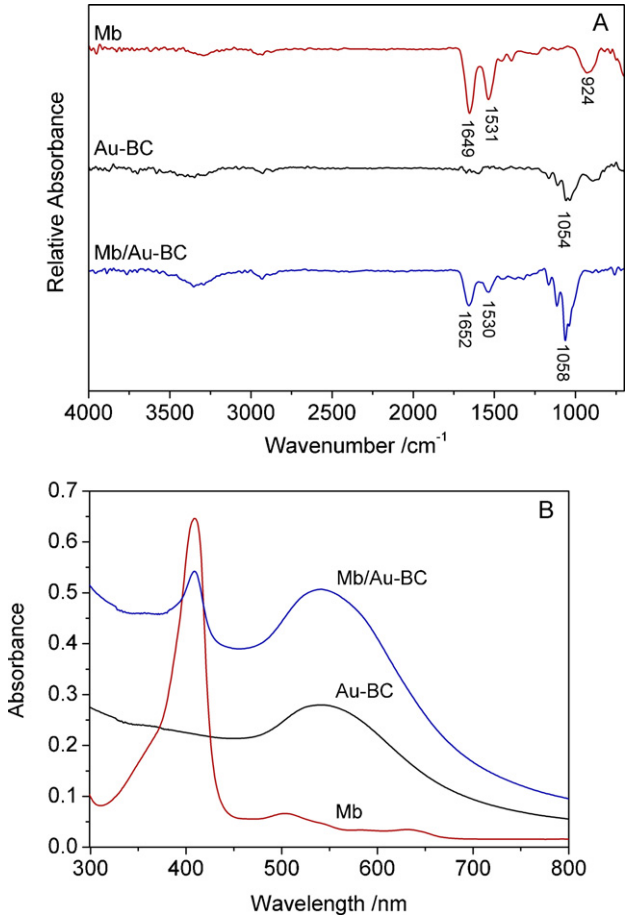

Fig. 3. (a) FT-IR spectra and (b) UV–vis spectra of Mb film, Au–BC film and Mb/Au–BC film.

rates in the range from 10 to 200 mV/s, which indicated that the electrochemical kinetics of the biosensor was a typical diffusion-controlled process. The similar phenomenon was also happened at Mb/Au–BC/GCE and HRP/Au–BC/GCE. From the results, it could be confirmed that a diffusion-controlled process occurred at the heme protein/Au–BC/GCE, and the reaction mechanism could be expressed as follows, which was also consistent with that reported in Refs. [37,38]:

$$\text{Heme protein (red)} + H_2O_2 \rightarrow \text{heme protein (Ox)} + H_2O$$

$$\text{Heme protein (Ox)} + \text{HQ (red)} \rightarrow \text{HQ (Ox)} + \text{heme protein (red)}$$

$$\text{HQ (Ox)} + 2H^+ + 2e \rightarrow \text{HQ (red)}$$

3.4. The characterizations of films by spectroscopy

Spectroscopic methods such as FT-IR and UV–vis spectroscopy were used to compare the structural variations of native and immobilized heme proteins on the film of Au–BC nanocomposite in Fig. 3. The shape and position of amide I (1600–1700 cm^{-1}) and amide II (1500–1600 cm^{-1}) of the IR bands provide detailed information on the secondary structure of the polypeptide chain and can be used as indicator of the conformational changes of proteins [39,40]. The amide I band at 1700–1600 cm^{-1} is caused by C=O stretching vibrations of the peptide linkage and the amide II band at 1600–1500 cm^{-1} results from a combination of N–H in-plane bending and C–N stretching of the peptide groups [39,40]. As shown in Fig. 3A, the spectra of the amide I and II bands of Mb in the Au–BC film (1652 and 1530 cm^{-1}) were nearly the same as those of Mb film (1649 and 1531 cm^{-1}), suggesting that Mb retained the essential features of its native structure on the Au–BC nanocomposite film. The similar behavior was observed on Hb and HRP also, indicating Au–BC nanocomposites could keep the bioactivity of heme proteins very well.

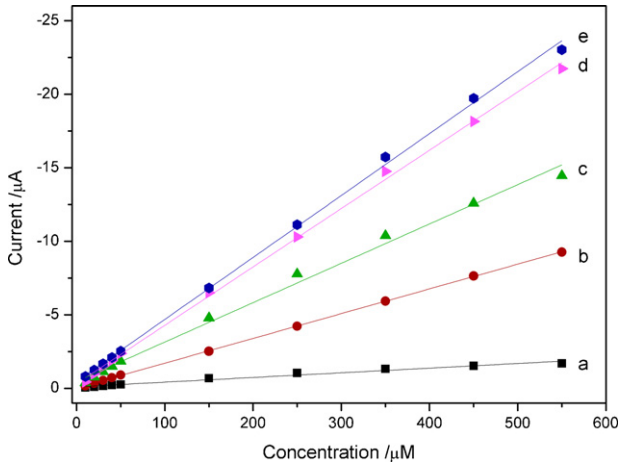

Fig. 4. Steady-state amperometric responses at the different HRP/Au–BC/GCE to the reduction of H_2O_2 in stirring phosphate buffer (pH 7.4) containing 0.5 mM HQ at the applied potential of −150 mV. The Au–BC nanocomposites were formed at different reaction times: (a) 0 min; (b) 5 min; (c) 10 min; (d) 30 min and (e) 60 min.

UV–vis spectroscopy is another useful tool for conformational studies of heme proteins since the positions of the Soret absorption band of heme can provide information about possible denaturation of heme proteins and particularly on the conformational change in the heme group region [41]. Fig. 3B showed the UV–vis spectra of Au–BC film, Mb film and Mb/Au–BC film. Au–BC nanocomposite had a broader peak from 520 nm to 580 nm, which was due to the surface plasmon coupling between closely spaced nanoparticles [42,43]. The UV–vis spectrum of native Mb gave a typical heme band at 409 nm (Fig. 3B), where Au–BC nanocomposite had no absorption. For the Mb/Au–BC film, except the broader peak caused by AuNPs, the absorption band corresponding to heme group was still observed at 409 nm. No obvious change was observed in the absorption peaks of Mb in the presence and absence of Au–BC nanocomposite, which indicated that Mb kept its natural structure in the mixture. The same results were obtained in the immobilization of Hb and HRP by Au–BC nanocomposite. Therefore, the heme proteins in Au–BC nanocomposite films retained their near native states, due to the good biocompatibility of Au–BC nanocomposite.

3.5. Influence of the amount of gold nanoparticles in Au–BC nanocomposite to the response of the developed biosensor

Since the amount of AuNPs in Au–BC nanocomposite might influence the conductivity of Au–BC nanocomposite and also the amount of heme proteins adsorbed by AuNPs, the amount of AuNPs in Au–BC nanocomposite might have an effect on the performance of the developed biosensor. HRP was used as an example to investigate the influence of the amount of AuNPs in Au–BC nanocomposite on the biosensor response in details. HRP was immobilized on the different Au–BC nanocomposites, which were synthesized at different reaction times. Fig. 4 showed the amperometric responses of the different HRP/Au–BC/GCE to the reduction of H_2O_2 under steady-state condition. The amount of AuNPs in Au–BC nanocomposite was influenced by the reaction time of the reduction of $HAuCl_4$ with PEI in aqueous mixed BC nanofibers solution. When the reaction time was 0 min, the electrode was modified by HRP/BC film actually. The lowest response to H_2O_2 was observed in the HRP/BC/GCE

(Fig. 4a). This phenomenon would be caused by the poor conductivity of BC which blocked the electron transfer from solution to electrode. According to Ref. [35], the surface concentration of AuNPs in nanocomposite increased with the reaction time and saturated after 1 h. As shown in Fig. 4, the magnitude of the steady-state current increased significantly with the increase of the amount of AuNPs on the BC surface and reached the maximum when the reaction time was 1 h, indicating the sensitivity of biosensor was related to the amount of AuNPs in Au–BC nanocomposite. The higher the amount of AuNPs in Au–BC nanocomposite, the higher the sensitivity of biosensor can be obtained. These results proved that AuNPs played an important role in the biosensor response. However, the response caused by HRP/Au/GCE was much smaller than that of HRP/Au–BC/GCE [35]. Therefore the better performance of HRP/Au–BC/GCE was attributed to the synergistic effect of AuNPs and BC in Au–BC nanocomposite. HRP could not only be entrapped by BC nano-network but also adsorbed by AuNPs. AuNPs acted as a bridge to link BC and HRP, and they could firmly immobilize HRP in the BC nano-network. In addition, as the merit of AuNPs with the high electrical conductivity and electron transfer accelerating capability, the non-conductivity of the BC could be compensated to some extent, which greatly improved the sensitivity of the biosensor. The Au–BC nanocomposite synthesized at the reaction time with 1 h was used for the following biosensing studies.

3.6. Optimization of experimental variables

The experimental parameters including pH and the applied potential were optimized for the analytical performance using HRP/Au–BC/GCE as a model.

The acidity of the solution has a significant effect on the bioactivity of enzymes. Therefore, the effect of the solution pH on the biosensor response in phosphate buffer containing 0.5 mM HQ and 100 μM H_2O_2 was examined (Fig. S2). The response currents increased from pH 5.0 to 6.0, remained stable between pH 6.0 and 8.0, and decreased above pH 8.0. The following experiments were performed at pH 7.4.

The influence of the applied potential on the current response to H_2O_2 was performed on HRP/Au–BC/GCE in 0.1 M stirring phosphate buffer containing 0.5 mM HQ and 30 μM H_2O_2 in the potential range of 0 to −0.3 V (Fig. S3). The biosensor response to H_2O_2 increased with the applied potential change from 0 to −0.15 V. The highest sensitivity was obtained at −0.15 V. Then a further increase of negative potential resulted in a little decrease in current response, which might be due to the fact that the potential of the reduction peak of HQ at HRP/Au–BC/GCE was near −0.15 V. Therefore −0.15 V was selected as the applied working potential for amperometric measurements. And at this relatively low potential, some interferents can be avoided.

3.7. Amperometric response and calibration curve to H_2O_2

Under the optimum conditions, a typical current–time plot of HRP/Au–BC/GCE on the successive addition of aliquot H_2O_2 was shown in Fig. 5A. As the H_2O_2 was added into the stirring buffer solution, the stepped increase of the amperometric current was observed. And the obvious increase of the current could be observed when the concentration of H_2O_2 was as low as 0.3 μM (the inset picture in Fig. 5A). The reduction current increased sharply to a stable value within 1 s by each addition, which was much faster than 2.5 s at HRP/AuNPs/sol–gel/gold electrode, 5 s at HRP–SiO_2/gold electrode and 10 s at HRP/magnetic dextran microsphere/GCE [14,37,38]. Such a fast response could be attributed to the cooperation of AuNPs and BC: first, the interconnected porous structure of BC did not inhibit mass transport. Second, AuNPs were favorable to the orientation of the HRP molecules on the electrode in the process of bioelectrocatalysis, and they transferred electrons more conveniently [14,38]. The corresponding calibration curve shown in Fig. 5B indicated that the hydrogen peroxide biosensor based on HRP exhibited a linear range of 0.3 μM to 1.0 mM (R^2 = 0.998), a sensitivity of 610 μA mM^{-1} cm^{-2} and a detection limit of 0.1 μM (S/N = 3). The H_2O_2 detection performances of the proposed biosensor were compared with those of HRP biosensors based on other matrices. The results were shown in Table 1. It showed that the HRP/Au–BC/GCE exhibited excellent performance in terms of a wider linear range and lower limit of detection for H_2O_2, suggesting the proposed biosensor based on Au–BC nanocomposite compared advantageously with respect to other biosensor designs.

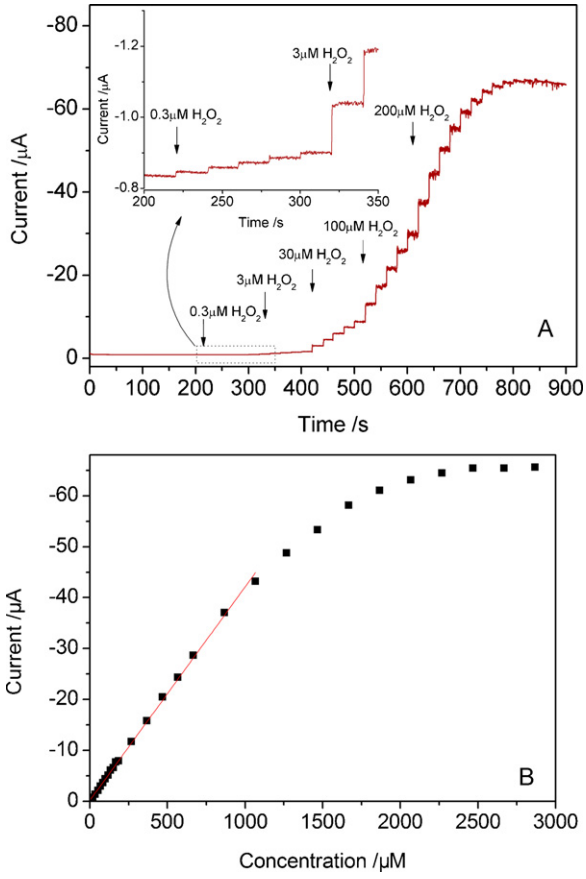

Fig. 5. (a) Amperometric response curves of HRP/Au–BC/GCE for successive additions of different concentrations of H_2O_2 in stirring phosphate buffer (pH 7.4) containing 0.5 mM HQ at the applied potential of −150 mV. The inset shows the amperometric response at time range from 200 s to 350 s. (b) Calibration curve of the current vs. the concentration of H_2O_2.

Mb/Au–BC and Hb/Au–BC films showed similar amperometric behavior with the injection of H_2O_2, but with much lower sensitivity (Fig. S4). The linear response ranges of Hb/Au–BC/GCE and Mb/Au–BC/GCE were from 10 μM to 1000 μM and 10 μM to 100 μM, and the detection limits were 3.9 μM and 5.1 μM, respectively. The different sensitivities of H_2O_2 obtained at heme protein based biosensor might be due to the different catalytic efficiencies of heme proteins to H_2O_2, which was similar to the behavior observed at heme protein–clay films [39].

3.8. Selectivity and stability of the biosensor

Selectivity and stability are two important factors in the performance of an enzyme sensor. Since HRP showed the highest sensitivity to H_2O_2, we investigated the selectivity and stability of HRP based biosensor in details. Several common electroactive com-

Table 1
Comparison of the analytical performance of this biosensor with that of some other H_2O_2 sensors.

Different H_2O_2 sensors	Linear range (mM)	Detection limit (μM)	Ref
HRP–SiO_2–modified Au electrode	0.02–0.20	3	[38]
HRP/AuNP–$CaCO_3$/silica sol–gel-modified GCE	0.04–8.0	1	[17]
HRP/SA[a]–PVB[b]/Au electrode	0.007–4.1	1.8	[44]
HRP/MSHS[c]/Nafion/GCE	0.0039–0.14	1.2	[45]
MWCNTs[d]/MG[e]/HRP/GCE	0.0005–0.02	0.5	[46]
HRP/CeO_2/chitosan/GCE	0.001–0.15	0.26	[47]
HRP/Organosilica@Chitosan/MWCNT/GCE	0.0007–2.8	0.25	[48]
Chitosan–CNTs[f]–NB[g]–HRP	0.001–0.24	0.12	[49]
HRP/BC–Au/GCE	0.0003–1.0	0.1	This work

[a] Sodium alginate.
[b] Polyvinyl butyral.
[c] Mesoporous silica hollow spheres.
[d] Multiwall carbon nanotubes.
[e] Methylene green.
[f] Carbon nanotubes.
[g] Nile blue.

pounds in real samples such as glucose, citric acid and uric acid were measured to examine whether they interfered with the determination of H_2O_2. 1 mM glucose, 1 mM citric acid and 1 mM uric acid were added sequentially in stirring 0.1 M phosphate buffer containing 0.5 mM HQ and 0.1 mM H_2O_2. The amperometric response (Fig. S5) remained unchanged after adding these interferents. The results showed that tenfold excess of glucose, citric acid and uric acid did not interfere with the detection of H_2O_2.

The electrode was stored in phosphate buffer (pH 7.4) at 4 °C when not in use. The stability of the biosensor under storage was investigated by measuring the amperometric response in 0.1 M phosphate buffer containing 0.5 mM HQ and 10 μM H_2O_2 every day. After 20 days storage, the biosensor still retained more than 87% of its original response to H_2O_2 (Fig. S6). Good long-term stability could be attributed to the strong interaction between HRP and Au–BC nanocomposite, which provided the encapsulated HRP a sheltered and biocompatible microenvironment that both prevented the loss of enzyme.

3.9. Real sample analysis

The applicability of the proposed biosensor was evaluated by detecting H_2O_2 in disinfector sample. The sample was diluted 20 times with pH 7.4 phosphate buffer solution, and the concentration of H_2O_2 contained in the diluted disinfector sample was tested using HRP based biosensor. The result was 47.7 ± 0.6 mM ($n = 3$). The result determined with potassium permanganate titrimetric method was 49.77 ± 0.03 mM ($n = 3$). As we can see, the results determined by the biosensor were satisfactory and agree closely with those measured by classical titrimetric method, indicating the biosensor could be used in practical analysis.

4. Conclusions

As a novel biocompatible nanocomposite, Au–BC nanocomposite was used for the immobilization of heme proteins with different sizes and biosensor fabrication successfully. Results showed that the Au–BC nanocomposite provided a biocompatible and conductive network structure to biomolecules, which could promote the electron transport, accelerate the mass transport and enhance the mechanical stability of the immobilization. Among these three H_2O_2 biosensors, HRP immobilized in the Au–BC film showed the highest biocatalytic activity with good sensitivity, low detection limit and fast response toward hydrogen peroxide. This unique nanocomposite material has widely potential applications in biosensors and biocatalysis.

Acknowledgement

This work was supported by the National Natural Science Foundation of China (Nos. 20805002, 90713013, 30890142, 50902002), the National Scientific Support Project 2009CB320305 (MOST, China) and the Scientific Research Foundation for the Returned Overseas Chinese Scholars, Ministry of Education.

Appendix A. Supplementary data

Supplementary data associated with this article can be found, in the online version, at doi:10.1016/j.talanta.2010.12.015.

References

[1] H. Zimmermann, A. Lindgren, W. Schuhmann, L. Gorton, Chem. Eur. J. 6 (2000) 592–599.
[2] E. Ferapontova, K. Schmengler, T. Borchers, T. Ruzgas, L. Gorton, Biosens. Bioelectron. 17 (2002) 953–963.
[3] G. Wang, J.J. Xu, H.Y. Chen, Z.H. Lu, Biosens. Bioelectron. 18 (2003) 335–343.
[4] S. Hrapovic, Y.L. Liu, K.B. Male, J.H.T. Luong, Anal. Chem. 76 (2004) 1083–1088.
[5] C.C. Chen, Y.S. Gu, Biosens. Bioelectron. 23 (2008) 765–770.
[6] Y.G. Liu, X.M. Feng, J.M. Shen, J.J. Zhu, W.H. Hou, J. Phys. Chem. B 112 (2008) 9237–9242.
[7] U. Narang, P.N. Prasad, F.V. Bright, K. Ramanathan, N.D. Kumar, B.D. Malhotra, M.N. Kamalasanan, S. Chandra, Anal. Chem. 66 (1994) 3139–3144.
[8] B.Q. Wang, B. Li, Q. Deng, S.J. Dong, Anal. Chem. 70 (1998) 3170–3174.
[9] J. Wang, Anal. Chim. Acta 399 (1999) 21–27.
[10] W. Jin, J.D. Brennan, Anal. Chim. Acta 461 (2002) 1–36.
[11] M.G. Zhang, A. Smith, W. Gorski, Anal. Chem. 76 (2004) 5045–5050.
[12] A.W. Shi, F.L. Qu, M.H. Yang, G.L. Shen, R.Q. Yu, Sens. Actuators B 129 (2008) 779–783.
[13] J. Shen, W. Wang, Q. Chen, M.S. Wang, S.Y. Xu, Y.L. Zhou, X.X. Zhang, Nanotechnology 20 (2009) 245307.
[14] J.B. Jia, B.Q. Wang, A.G. Wu, G.J. Cheng, Z. Li, S.J. Dong, Anal. Chem. 74 (2002) 2217–2223.
[15] J. Li, J.D. Qiu, J.J. Xu, H.Y. Chen, X.H. Xia, Adv. Funct. Mater. 17 (2007) 1574–1580.
[16] J. Njagi, S. Andreescu, Biosens. Bioelectron. 23 (2007) 168–175.
[17] W.Y. Cai, Q. Xu, X.N. Zhao, J.H. Zhu, H.Y. Chen, Chem. Mater. 18 (2006) 279–284.
[18] Y. Liu, J.P. Lei, H.X. Ju, Talanta 74 (2008) 965–970.
[19] D. Klemm, D. Schumann, U. Udhardt, S. Marsch, Prog. Polym. Sci. 26 (2001) 1561–1603.
[20] M. Tabuchi, K. Kobayashi, M. Fujimoto, Y. Baba, Lab. Chip 5 (2005) 1412–1415.
[21] M. Shoda, Y. Sugano, Biotechnol. Bioprocess Eng. 10 (2005) 1–8.
[22] A. Svensson, E. Nicklasson, T. Harrah, B. Panilaitis, D.L. Kaplan, M. Brittberg, P. Gatenholm, Biomaterials 26 (2005) 419–431.
[23] X. Li, S.Y. Chen, W.L. Hu, S.K. Shi, W. Shen, X. Zhang, H.P. Wang, Carbohydr. Polym. 76 (2009) 509–512.
[24] J.D. Fontana, A.M. Desouza, C.K. Fontana, I.L. Torriani, J.C. Moreschi, B.J. Gallotti, S.J. Desouza, G.P. Narcisco, J.A. Bichara, L.F.X. Farah, Appl. Biochem. Biotechnol. 24–5 (1990) 253–264.
[25] E.J. Vandamme, S. De Baets, A. Vanbaelen, K. Joris, P. De Wulf, Polym. Degrad. Stab. 59 (1998) 93–99.
[26] H. Yano, J. Sugiyama, A.N. Nakagaito, M. Nogi, T. Matsuura, M. Hikita, K. Handa, Adv. Mater. 17 (2005) 153–155.
[27] W.K. Czaja, D.J. Young, M. Kawecki, R.M. Brown, Biomacromolecules 8 (2007) 1–12.

[28] Y. Liang, P. He, Y.J. Ma, Y. Zhou, C.H. Pei, X.B. Li, Electrochem. Commun. 11 (2009) 1018–1021.
[29] K.R. Brown, A.P. Fox, M.J. Natan, J. Am. Chem. Soc. 118 (1996) 1154–1157.
[30] I. Willner, B. Willner, E. Katz, Bioelectrochemistry 70 (2007) 2–11.
[31] A.L. Crumbliss, S.C. Perine, J. Stonehuerner, K.R. Tubergen, J.G. Zhao, R.W. Henkens, Biotechnol. Bioeng. 40 (1992) 483–490.
[32] J.M. Pingarron, P. Yanez-Sedeno, A. Gonzalez-Cortes, Electrochim. Acta 53 (2008) 5848–5866.
[33] A.N. Shipway, M. Lahav, I. Willner, Adv. Mater. 12 (2000) 993–998.
[34] J.F. Hicks, F.P. Zamborini, A. Osisek, R.W. Murray, J. Am. Chem. Soc. 123 (2001) 7048–7053.
[35] T. Zhang, W. Wang, D. Zhang, X. Zhang, Y. Ma, Y. Zhou, L. Qi, Adv. Funct. Mater. 20 (2010) 1152–1160.
[36] D.Y. Zhang, L.M. Qi, Chem. Commun. (2005) 2735–2737.
[37] H.L. Zhang, G.S. Lai, D.Y. Han, A.M. Yu, Anal. Bioanal. Chem. 390 (2008) 971–977.
[38] S. Yang, W.Z. Jia, Q.Y. Qian, Y.G. Zhou, X.H. Xia, Anal. Chem. 81 (2009) 3478–3484.
[39] Y.L. Zhou, N.F. Hu, Y.H. Zeng, J.F. Rusling, Langmuir 18 (2002) 211–219.
[40] S. George, H.K. Lee, J. Phys. Chem. B 113 (2009) 15445–15454.
[41] J.F. Rusling, A.E.F. Nassar, J. Am. Chem. Soc. 115 (1993) 11891–11897.
[42] K.H. Su, Q.H. Wei, X. Zhang, J.J. Mock, D.R. Smith, S. Schultz, Nano Lett. 3 (2003) 1087–1090.
[43] S.Z. Zhang, W.H. Ni, X.S. Kou, M.H. Yeung, L.D. Sun, J.F. Wang, C.H. Yan, Adv. Funct. Mater. 17 (2007) 3258–3266.
[44] C.H. Liu, X.L. Guo, H.T. Cui, R. Yuan, J. Mol. Catal. B: Enzyme 60 (2009) 151–156.
[45] Z.X. Cao, J. Zhang, J.L. Zeng, L.X. Sun, F. Xu, Z. Cao, L. Zhang, D.W. Yang, Talanta 77 (2009) 943–947.
[46] A.K. Upadhyay, T.W. Ting, S.M. Chen, Talanta 79 (2009) 38–45.
[47] X.L. Xiao, Q.F. Luan, X. Yao, K.B. Zhou, Biosens. Bioelectron. 24 (2009) 2447–2451.
[48] S.H. Chen, R. Yuan, Y.Q. Chai, B. Yin, W.J. Li, L.G. Min, Electrochim. Acta 54 (2009) 3039–3046.
[49] F.N. Xi, L.J. Liu, Z.C. Chen, X.F. Lin, Talanta 78 (2009) 1077–1082.